Journal of Ceramic Processing Research. Vol. 8, No. 2, pp. 91~97 (2007)

J O U R N A L O F
Ceramic Processing Research

Sintering behavior and mechanical properties of binderless WC-TiC produced by pulsed current activated sintering

Hwan-Cheol Kim, Dong-Ki Kim, In-Yong Ko and In-Jin Shon*

Department of Advanced Materials Engineering, Research Center of Advanced Materials Development, Engineering Research Institute, Chonbuk National University, Jeonbuk 561-756, Korea

Pulsed current activated sintering (PCAS) is utilized to consolidate ultra-fine grain WC-*x*at.%TiC (*x*=0-50) cemented carbides. Densification to near theoretical density in a relatively short time can be accomplished without significant change in the grain size. WC-50at.%TiC with a relative density of up to 99% was produced within 5 minutes with the simultaneous application of 60 MPa pressure. The average grain sizes of the densified materials were about 200 nm. The sintered WC-20at.%TiC material had fracture toughness and hardness values of 7.5 MPa·m$^{1/2}$ and 2240 kg/mm^2, respectively.

Key words: Rapid Sintering, Pulsed Current Activated Sintering, WC-TiC, Hard Materials, Microstructure, Hardness, Fracture Toughness.

Introduction

Tungsten carbide hard materials are widely used for a variety of machining, cutting, drilling, and other applications. Morphologically, they consist of a high volume fraction of the "hard" hexagonal WC phase embedded within a soft and tough Co or Ni binder phase [1]. WC-Co and WC-Ni hard materials can be densified by liquid phase sintering and the mechanical properties of these materials depend on their composition, and microstructure (especially on the grain size of the carbide phase [2]). Thus, the control of grain growth of the carbide phase during liquid phase sintering is an important objective. But, these binder phases are inferior to the carbide phase in chemical characteristics; corrosion and oxidation start in the binder phase first [3]. Hence, the development of WC-TiC binderless cemented carbides has been applied in mechanical seals and sliding parts due to their enhanced corrosion resistance. Characteristic of this system is the high hardness of its components (TiC has 31 GPa Vickers hardness and WC has 25 GPa), which facilitates its uses as abrasives, cutting and polishing tools among others [4]. Also, TiC has been used as a carbide-binder because it forms a WC-TiC solid solution phase [5].

Since property improvements can also be effected through microstructural changes (notably by grain size refinement [6, 7]), the focus has shifted to improvements in processing methods. However, preparation and processing of cemented carbides having a refined grain structure can result in residual porosity attributed to localized agglomeration of the powders [8]. Additionally, even when fine grain powders (e.g., nanopowders) are used as starting materials, conventional methods to consolidate them often result in substantial grain growth [9]. To minimize grain growth, it is necessary to achieve consolidation at as a low a temperature as possible. In this regard, the spark plasma sintering (SPS) method has been shown to be effective in achieving this goal [10, 11]. Recently the pulse current activated sintering (PCAS) technique has been shown to be effective in the sintering of nanostructured materials in very short times (typically within 2 minutes) [12, 13]. This method combines a short time, high-temperature exposure with pressure application. During the PCAS process, a large current will be induced in the sample and in the graphite die. As a result, the sample can be sintered uniformly and rapidly. In this study, we report results on the sintering of binderless WC-TiC hard materials by a rapid sintering process, pulsed current activated sintering (PCAS) method which combines induced current with high-pressure application. The goal of this study is to produce dense, ultra-fine WC-*x*at.%TiC (*x*=0-50) hard materials in very short sintering times (<5 minutes). And we investigated the effect of TiC contents on the mechanical properties of WC-TiC hard materials.

Experimental Procedure

The tungsten carbide powder used in this research was supplied by TaeguTec Ltd. (Taegu, Korea). The powder had a grain size of 0.4 μm measured by a Fisher sub-sieve sizer (FSSS) and was reported to be 99.5% pure. Nano-sized TiC powder obtained from Nanostructured and Amorphous Materials, Inc. (Houston,

*Corresponding author:
Tel : +82-63-270-2381
Fax: +82-63-270-2386
E-mail: ijshon@chonbuk.ac.kr

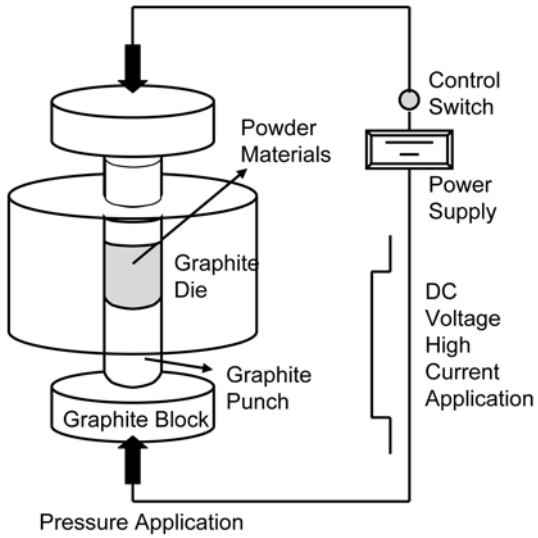

Fig. 1. Schematic diagram of apparatus for pulsed current activated sintering.

TX, USA) was used. The powder had a grain size of 70 nm measured by specific surface area (SSA) and was reported to be 99% pure. All powders were milled in a Universal Mill with a ball-to-powder weight ratio of 6:1. Milling was done in polyethylene bottles using tungsten carbide balls and was performed at a horizontal rotation velocity of 250 rpm for 24 h.

The powders were placed in a graphite die (outside diameter, 45 mm; inside diameter, 20 mm; height, 40 mm) and then introduced into the pulsed current activated sintering system made by Eltek Co. in the Republic of Korea. A schematic diagram of this method is shown in Fig. 1. The PCAS apparatus includes an 18 V, 2800 A DC power supply (which provides a pulsed current with 20 μs on time and 10 μs off time through the sample and die) and a 50 kN uniaxial press. The system was first evacuated and a uniaxial pressure of 60 MPa was applied. A DC current was then activated and maintained until the densification rate was negligible, as indicating by the observed shrinkage of the sample. Sample shrinkage is measured in real time by a linear gauge measuring the vertical displacement. Temperatures were measured by a pyrometer focused on the surface of the graphite die. Depending on heating rate, the electrical and thermal conductivities of the compact, and on its relative density, a difference in temperature between the surface and the center of the sample exists. The heating rates were approximately 900 K·minute^{-1} in the process. At the end of the process, the induced current was turned off and the sample was allowed to cool to room temperature. The entire process of densification using the PCAS technique consi1sts of four major control stages. These are chamber evacuation, pressure application, power application, and cool down. The four major stages in the sintering are shown schematically in Fig. 2. The process was carried out under a vacuum of 40 mTorr (5.33 Pa).

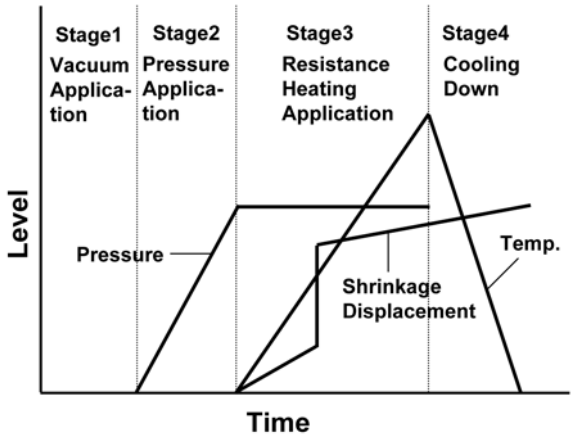

Fig. 2. Schematic representation of the temperature, pressure and shrinkage displacement profiles during PCAS.

The relative densities of the sintered samples were measured by the Archimedes method. Microstructural information was obtained from product samples, which had been polished and fractured at room temperature. Compositional and microstructural analyses of the products were made through X-ray diffraction (XRD), scanning electron microscopy (SEM) with energy dispersive spectroscopy (EDS) and field-emission scanning electron microscopy (FE-SEM). Vickers hardness was measured by performing indentations at a load of 10 kg_f and with a dwell time of 15 s. The carbide grain size, d_{wc} was obtained by the linear intercept method [14, 15].

Vickers hardness measurements were made on polished sections of the binderless WC-TiC hard materials using a 30 kg_f load and 15 s dwell time. Indentations with large enough loads produced radial cracks emanating from the corners of the indent. Fracture toughness was calculated from cracks produced in indentations under large loads. The length of these cracks permits an estimation of the fracture toughness of the material by means of the Anstis et al. expression [16]:

$$K_{IC}=0.016(E/H)^{1/2}P/C^{3/2} \quad (1)$$

where E is Young's modulus, H the indentation hardness, P the indentation load, and C the trace length of the crack measured from the center of the indentation. As in the case of hardness values, the toughness values are derived from the average of ten measurements.

Results and Discussion

The variations of shrinkage displacement and temperature of the surface of the graphite die with heating time for various TiC contents during the sintering of WC-TiC samples using pulsed current activated sintering with 2800 A pulsed DC under a pressure of 60 MPa pressure are shown in Fig. 3. In all cases, initially the sample exhibits an increase in volume due to thermal expansion. As the electric current is applied,

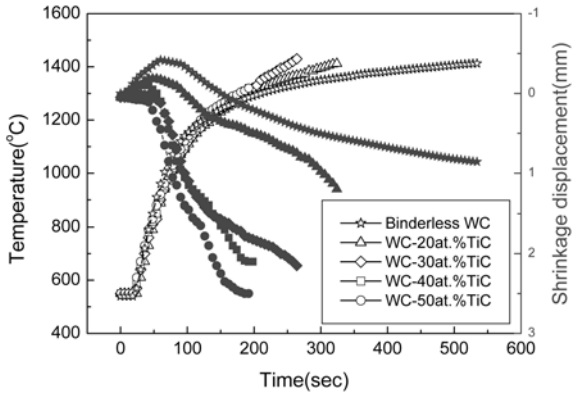

Fig. 3. Variations of temperature and shrinkage displacement with heating time during high-frequency induction heated sintering of WC-*x*at.%TiC hard materials (under 60 MPa pressure, 2800A).

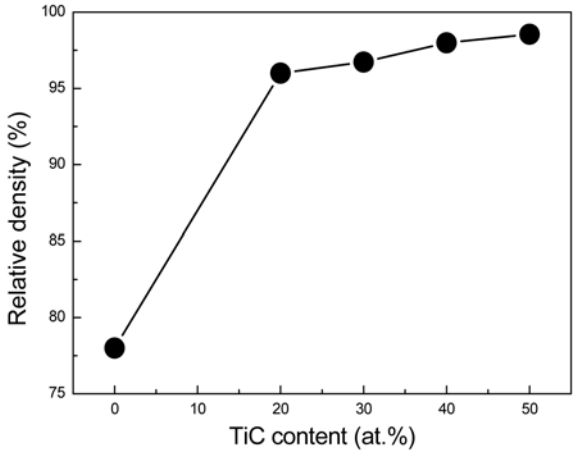

Fig. 4. Relative density of binderless WC-*x*at.%TiC hard materials produced by PCAS.

the shrinkage displacement increased with temperature up to about 1200°C in the case of binderless WC. When the temperature reaches about 1400 °C, the densification rate becomes nearly negligible, and as will be seen later, the samples of binderless WC have densified to 78% of theoretical density in about 500 s. In the case of additions of TiC, however, the onset of shrinkage took place at about 950-1100 °C. The observation of the onset of sintering was affected by the content of TiC. On increasing the TiC content, the sintering temperature was decreased. It was thought that TiC was acted as a carbide-binder because it forms WC-TiC solid solution phase [5]. The dependence of relative density of the WC-TiC hard materials on TiC content for samples produced by the PCAS method is shown in Fig. 4. In the absence of a TiC additive, WC can be sintered, but its density under the same experimental conditions is low (~78%). However, in the presence of 20at.% TiC, the density increases to 96%, and it increases further to 98.5% as the amount of TiC is increased to 50at.%. With increasing TiC content, the relative density of WC-TiC composites increased.

The nature of the products of sintering is revealed in

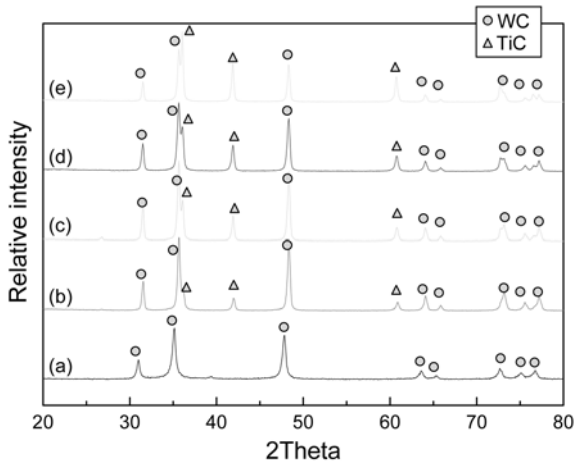

Fig. 5. XRD patterns of WC-*x*at.%TiC composite sintered by PCAS (a) WC, (b) WC-20at.%TiC, (c) WC-30at.%TiC, (d) WC-40at.%TiC and (e) WC-50at.%TiC.

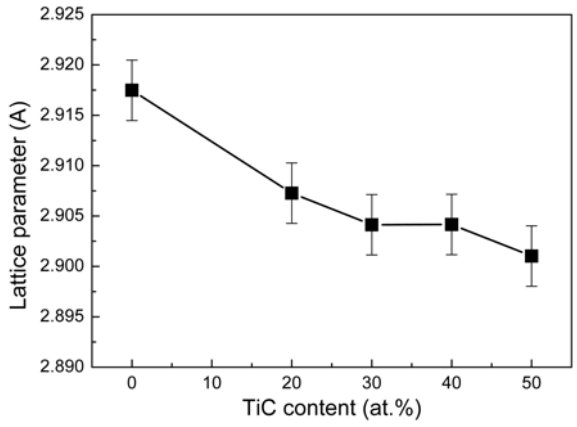

Fig. 6. Plot of WC phase lattice parameter as a function of TiC content produced by PCAS (Error bars=0.5%).

Fig. 5, which shows the XRD patterns of WC and WC-TiC hard materials after sintering by PCAS in this study. In the case of pure WC, only peaks belonging to WC are seen, indicating that no compositional changes took place during the sintering. No peaks for the subcarbide W_2C or any impurity phase are present. In the case of WC-TiC hard materials, only WC and TiC peaks were observed. In XRD patterns of products, we could not find the peaks of solid solution, known as (W,Ti)C [5], because solid solution peaks overlapped with that of TiC. So we calculated the lattice parameter, *a*, of WC using the XRD results. Figure 6 shows the calculated lattice parameter of WC with different content of TiC. On increasing the TiC content, a decrease in the WC lattice parameter was observed. It is thought that parameter-composition curve indicates the formation of solid solution series. There is a peak shift corresponding to the change in the WC:TiC ratio in Fig. 5.

SEM images of etched surfaces of WC and fractured surfaces of WC-TiC samples sintered by PCAS under a pressure of 60 MPa are shown in Fig. 7. In the case of binderless WC, when the temperature was raised to

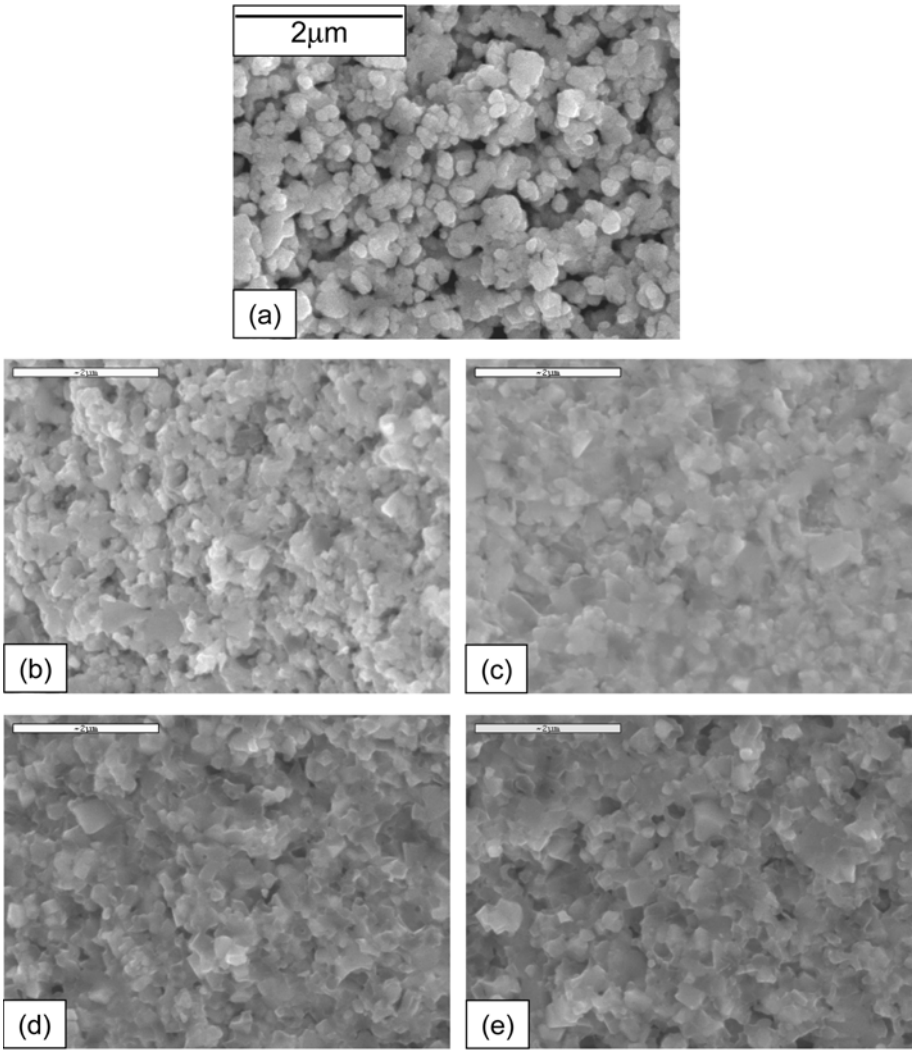

Fig. 7. SEM images of fracture surfaces of WC-*x*at.%TiC composites sintered by PCAS (a) WC, (b) WC-20at.%TiC, (c) WC-30at.%TiC, (d) WC-40at.%TiC and (e) WC-50at.%TiC.

1400 °C, the powders sintered producing porous and non-faceted products. In the case of WC-TiC hard materials, however, SEM images of their microstructures revealed dense materials with a uniform distribution of the carbide phases and a narrow grain size distribution. In contrast to the spherical shape of the starting or milled powder particles, the grains of the sintered WC are highly faceted with relatively high aspect ratios. No evidence of another phase can be seen, in agreement with the XRD results. The development of well-defined crystallographic facets during sintering of WC reflects the difference in surface energy of the (010) and (100) planes. Because of this anisotropy, WC grains tend to attain a triangular prism shape, as has been observed before [17]. From the fracture surfaces, it is difficult to distinguish the WC and TiC phases. The grain morphology and different phases present in the microstructures were studied using an back-scattered electrons in FE-SEM, see Fig. 8. In the case of pure WC, only WC phase and micro-pores were observed. In the cases of WC-TiC hard materials, however, two phases appearing white and gray were observed. It is confirmed that the white phase was WC and the gray phase was TiC, respectively, as shown in Fig. 9. The average WC grain size of WC-TiC (under 60 MPa, 90% output) determined by the linear intercept method was about 200 nm. On increasing the TiC content, the volume fraction of gray parts increased. In this figure, we could not find a typical core-rim microstructure of solid solution because of the absence of binder. At the sintering temperatures of carbides, around 1450 °C, WC-TiC may form the mixed carbide (W,Ti)C plus free carbon [18]. For a conventional cemented carbide, the free C resulting from the dissolution of WC in TiC may be dissolved in the Co binder [19]. In the binderless cemented carbide studied in this study, however, there is no cobalt phase. This may be a result of the free carbon in the grain boundary, as shown in Fig. 9. The attainment of higher density and finer structure in a short time using induced current heating with pressure is not well understood. However, we would suggest that the accelerated PCAS densification may be attributed to a combination of

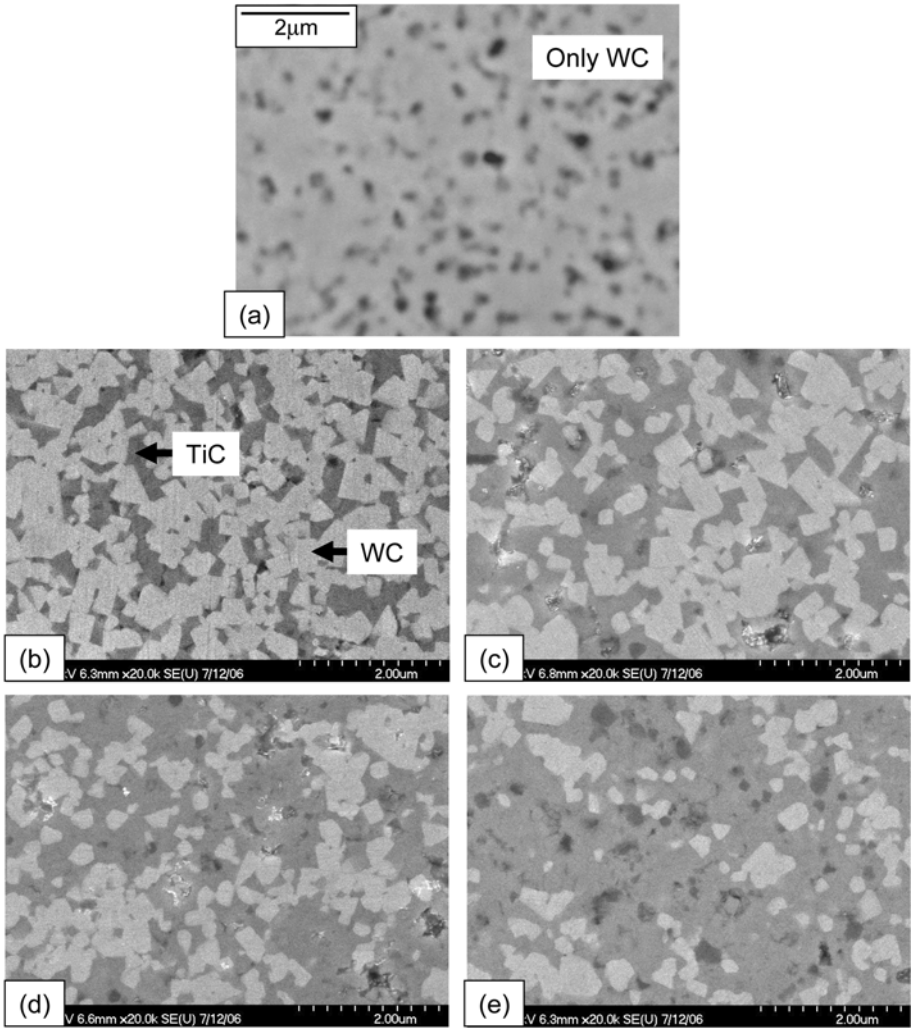

Fig. 8. Back-Scattered Electron FE-SEM images of of WC-*x*at.% TiC composites sintered by PCAS (a) WC, (b) WC-20at.%TiC, (c) WC-30at.%TiC, (d) WC-40at.%TiC and (e) WC-50at.%TiC.

electrical discharge, resistance heating, and pressure application effects. When the electric current is applied, energy emission may be concentrated at particle contacts that attain high temperatures. These concentrated heat effects at particle surfaces may cause surface melting and oxide breakdown, similar to surface effects in the electrodischarge machining (EDM) process [20]. PCAS methods have short-time high-temperature exposure with high-pressure applications. The role of the current in sintering and or synthesis has been the focus of several attempts aimed at providing an explanation of the observed enhancement of sintering and improved characteristics of the product. An example of the latter is the observation of clean boundaries in ceramics sintered by the PCAS method relative to those obtained by conventional methods. The role played by the current has been variously interpreted, the effect being explained in terms of the fast heating rate due to Joule heating, the presence of a plasma in the pores separating powder particles, and the intrinsic contribution of the current to mass transport. So we would suggest that the accelerated PCAS densification may be attributed to a combination of fast heating rates and intrinsic effects on mass transport.

Vickers hardness measurements were made on polished sections of the binderless WC-TiC hard materials using a 30 kg_f load and 15 s dwell time. Indentations with large enough loads produced radial cracks emanating from the corners of the indent. The calculated hardness values and fracture toughness values of binderless WC and WC-TiC composites are shown in Fig. 10 as a function of TiC content for samples produced by PCAS. The binderless WC hard materials had the lowest hardness value due to their lower relative density of 78%. The hardness and toughness values were improved by the addition of TiC. The hardness and fracture toughness values of WC-20at.%TiC with WC about 0.2 μm in size when made by PCAS were 2240 kg/mm^2 and 7.5 $MPa \cdot m^{1/2}$, respectively. In the case of further additions of TiC, the Vickers hardness and the fracture toughness decreased with increasing TiC content. These results were different from those of other researchers. Lee et al. [21] reported that the hardness of WC-TiC-10wt.%Co

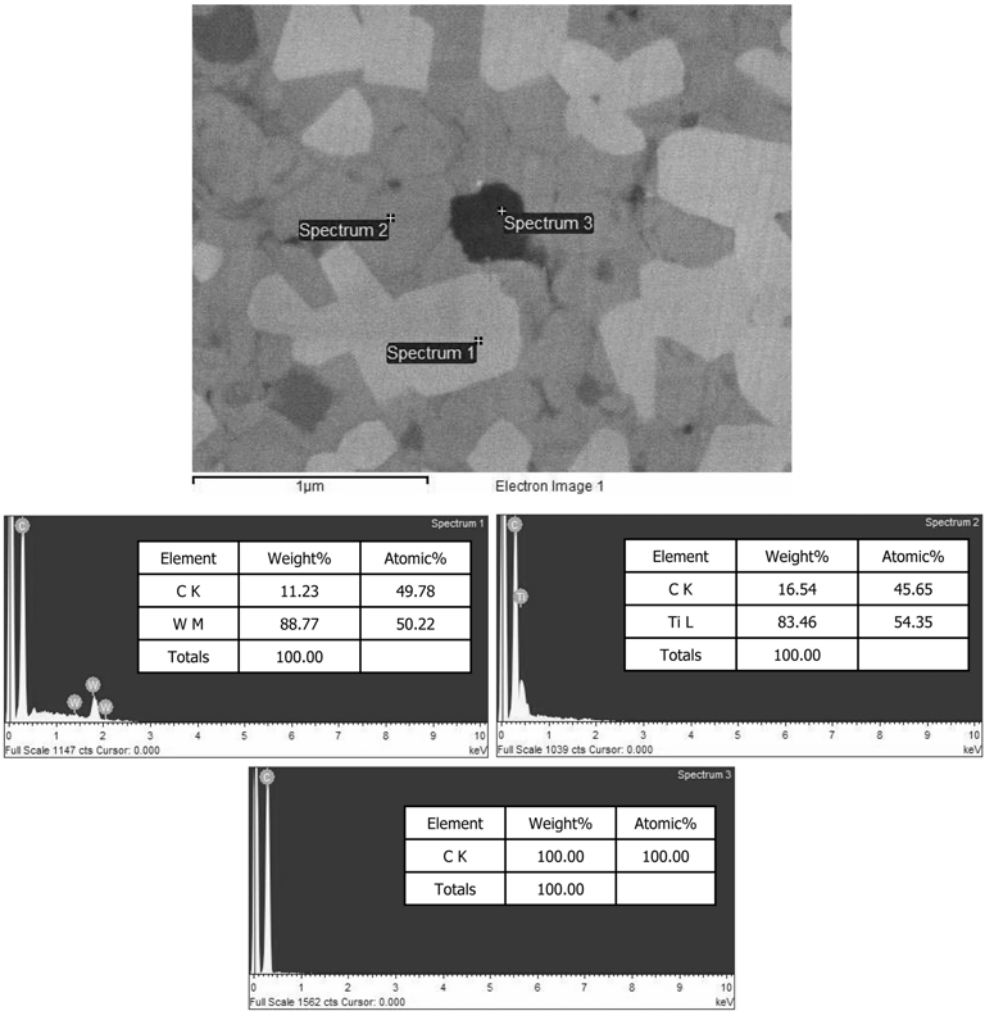

Fig. 9. Enlarged FE-SEM image and EDS data of WC-50at.%TiC composite sintered by PCAS.

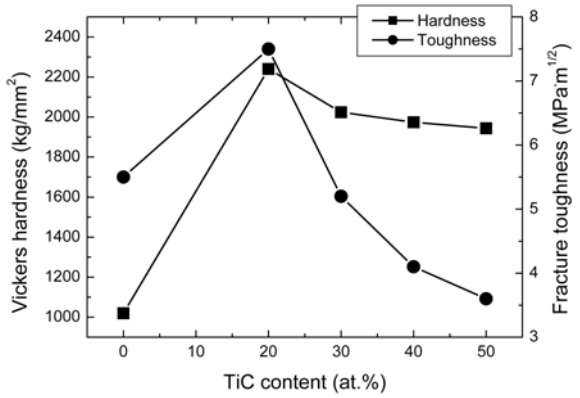

Fig. 10. Vickers hardness and fracture toughness of WC-*x*at.%TiC hard materials sintered by PCAS.

cemented carbides increased with increasing TiC content and with decreasing WC grain size. They said that as the hardness of TiC/(Ti, W)C core-rim phase is higher than that of the WC phase, the hardness of WC-TiC-10wt.%Co cemented carbide increases due to an increased amount of core-rim phase with increasing TiC content [21]. The existence of even a small amount of Co in the grain boundaries is believed to be of crucial importance to both the sintering process as well as to the mechanical properties of the densified material. Much of the reduced mechanical properties of binderless cemented carbides with TiC contents in this study may be explained by the existence of carbon in the grain boundaries. In the case of WC-TiC-Co, the free C resulting from the dissolution of WC in TiC may be dissolved in the Co binder. In a binderless carbide, however, no Co but a large amount of free carbon was found [22]. These C-rich phases are likely to reduce the mechanical properties of this binderless carbide.

Summary

Using pulsed current activated sintering (PCAS), the densification of WC-*x*at.%TiC hard materials with a grain size of 200 nm were accomplished using ultra fine powders of WC and TiC. A complete densification of the materials was achieved within 5 minutes. The relative density of the composite was about 98.5% for an applied pressure of 60 MPa and a pulsed DC current of 2800 A. The addition of TiC results in a higher density

and mechanical properties. hihger the lowest hardness value due to the lower density. incrased to 50at.% low (~78%). The Vickers hardness and the fracture toughness decreased with increasing the TiC content above 20at.%. The hardness and fracture toughness values of WC-20at.%TiC with WC about 0.2 μm in size when made by PCAS were 2240 kg/mm^2 and 7.5 MPa·m$^{1/2}$, respectively, for 60 MPa and a pulsed DC current of 2800 A.

Acknowledgements

This work was supported by the grant of Post-Doc. Program, Chonbuk National University (2006).

References

1. K. Mohan and P.R. Strutt, Nano Structured Mater. 7 (1996) 547-555.
2. B.K. Kim, G.H. Ha, and D.W. Lee, J. Mater. Proce. Tech. 63 (1997) 317-321.
3. H.E. Exner, in "Physical and Chemical Nature of Cemented Carbide" (Int. Met. Rev, 1979) p. 149.
4. K.J.A. Brooks, in "Cemented Carbide for Engineers and Tool Users" (East Barnet: Int. Carbide Data, 1983) p. 1.
5. S. Imasato, K. Tokumoto, T. Kitada, and S. Sakaguchi, Int. J. Refract. Met. & Hard Mater. 13 (1997) 305-312.
6. H. Gleiter, Progress in Mater. Sci. 33 (1989) 223-315.
7. G.E. Fougere, J.R. Weertman, R.W. Siegel, and S. Kim, Scripta Metallurgica et Materialia 26 (1992) 1879-1883.
8. T.S. Srivatsan, R. Woods, M. Petraroli, and T.S. Sudarshan, Powder Tech. 122 (2002) 54-60.
9. R.B. Schwarz, S.R. Srinivasan, J.J. Petrovic, and C.J. Maggiore, Mater. Sci. Eng. A 155 (1992) 75-83.
10. M. Omori, Mater. Sci. Eng. A 287 (2000) 183-188.
11. S.I. Cha and S.H. Hong, Mater. Sci. Eng. A 356 (2003) 381-389.
12. H.C. Kim, I.J. Shon, J.E. Garay, and Z.A. Munir, Int. J. Refract. Met. & Hard Mater. 22 (2004) 257-264.
13. H.C. Kim, I.J. Shon, J.K. Yoon, and J.M. Doh, Int. J. Refract. Met. & Hard Mater. 25 (2007) 46-52.
14. ASTM E112-96e2.
15. J.H. Han and D.Y. Kim, Acta Mater. 46 (1998) 2021-2028.
16. G.R. Anstis, P. Chantikul, B.R. Lawn, and D.B. Marshall, J. Am. Ceram. Soc. 64 (1981) 533-538.
17. A.V. Shatov, S.A. Firstov, and I.V. Shatova, Mater. Sci. Eng. A 242 (1998) 7-14.
18. H.E. Exner, Int. Metals Rev. 4 (1979) 149-173.
19. G. Wirmark and G.L. Dunlop, in "Phase transformations in the binder phase of Co-W-C cemented carbides" (Science of hard materials, 1983) p. 1.
20. J. Fleischer, T. Masuzawa, J. Schmidt, and M. Knoll, J. Mater. Proce. Tech. 149 (2004) 246-249.
21. K.H. Lee, S.I. Cha, B.K. Kim, and S.H. Hong, Int. J. Refract. Met. Hard Mater. 24 (2006) 109-114
22. T.S. Srivatsan, M.R. Woods, M. Petraroli, and T.S. Sudarshan, Powder Tech. 122 (2002) 54-60.